Electronic Supplementary Material (ESI) for Dalton Transactions.

SUPPORTING INFORMATION

A biophysical study of the interactions of palladium(II), platinum(II) and gold(III) complexes of aminopyridyl-2,2'-bipyridine ligands with RNAs and other nucleic acid structures

Francesca Binacchi, Cassandra Elia, Damiano Cirri, Corjan van de Griend, Xue-Quan Zhou, Luigi Messori, Sylvestre Bonnet, Alessandro Pratesi, Tarita Biver

Table of Contents

Formation of the RNA 4WJ: melting test 2
Spectrophotometric characterisation of the metal complexes 3
Poly(rA)2poly(rU) absorbance titrations 8
Melting Tests 9
Poly(rA)poly(rU) Ethidium displacement 10
DNA Absorbance titrations 11
DNA Ethidium displacement and viscometric tests 12
Circular Dichroism spectra of $[Pd(H_2L1)]Cl_2$/DNA and $[Pt(H_2L1)]Cl_2$/DNA 13
G-quadruplex absorbance titrations 14
G-quadruplex ESI mass spectra 15
RNA-4WJ absorbance titrations 17
RNA-4WJ melting tests 18

Formation of the RNA 4WJ: melting test

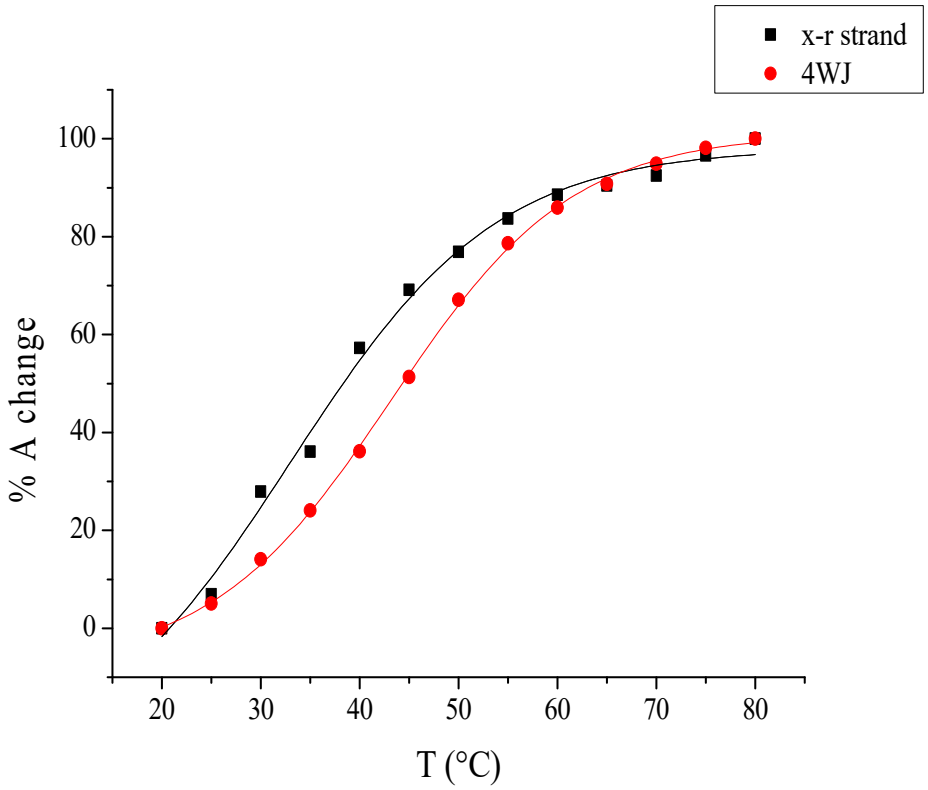

Figure S1. UV-melting tests of the coupled x-r strands and of the RNA 4WJ; $C_{x\text{-}r\ strand} = C_{4WJ} = 1.03 \times 10^{-5}$ M; C_{CaCl2} = 182 µM. % A change = 100*(A – A°)/(A$^{\infty}$ – A°) where A° and A$^{\infty}$ are the two absorbance values limiting the fitting sigmoid.

Spectrophotometric characterisation of the metal complexes

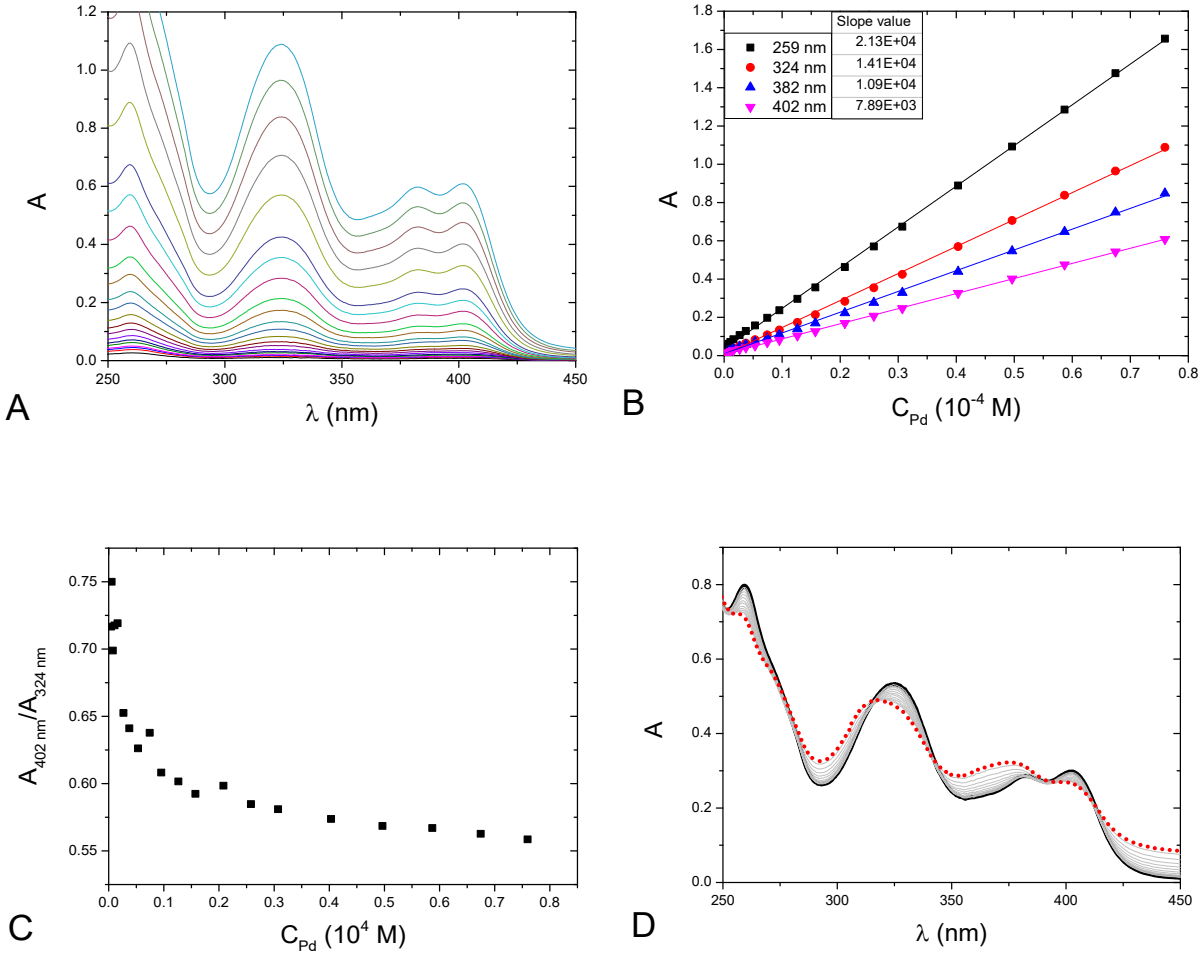

Figure S2. [Pd(H_2L1)]Cl_2: absorbance spectra at different concentrations (A) C_{Pd} from 0 M to 7.60×10^{-5} M with relevant absorbance versus concentration plot (B) and absorbance ratio plot (C), 25.0 °C; (D) absorbance spectra in the 25 °C (—) – 90 °C (.....) temperature range, C_{Pd} = 2.08×10^{-5} M. NaCl 0.1 M, NaCac 2.5 mM, pH = 7.0.

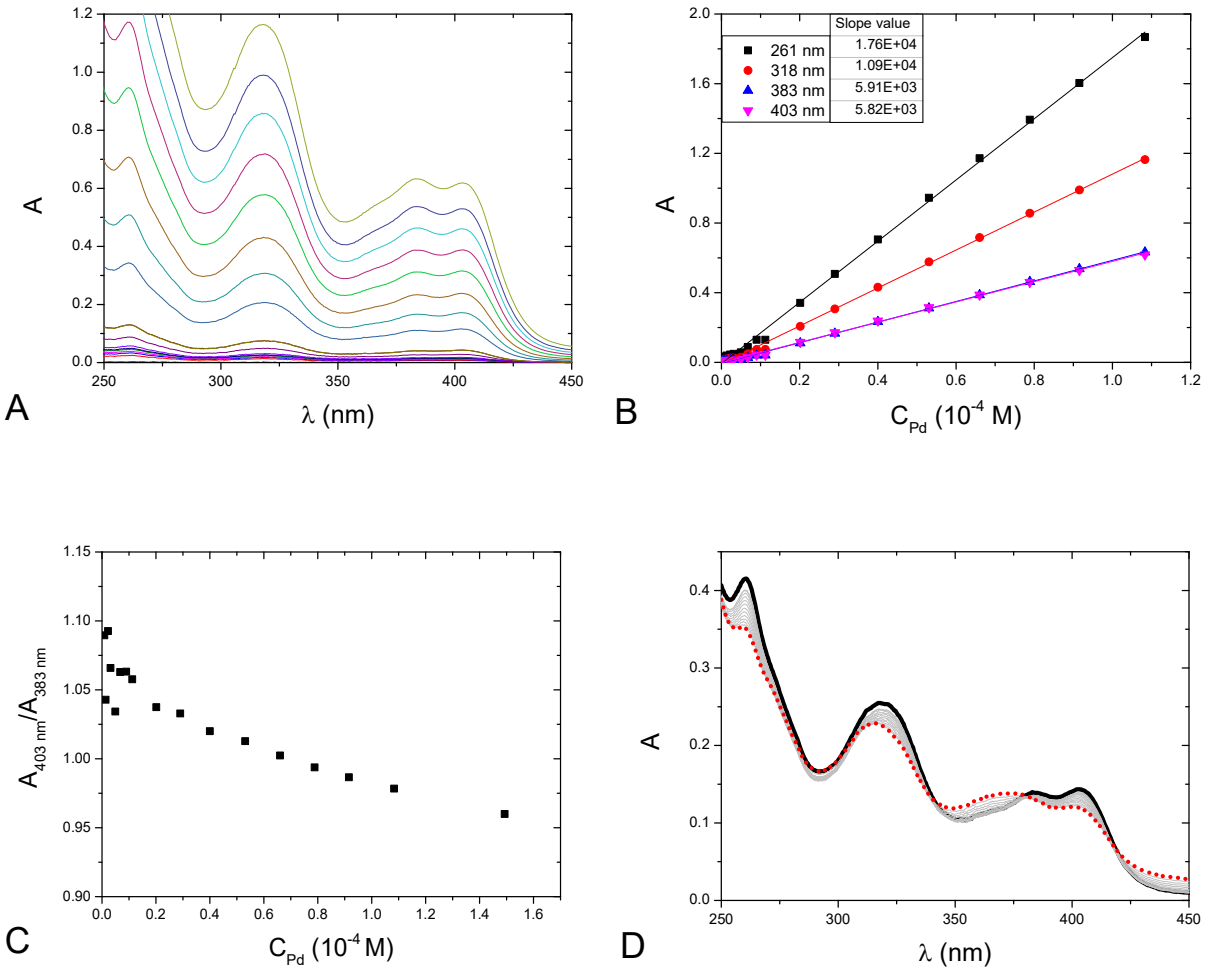

Figure S3. $[Pd(H_2L2)]Cl_2$: absorbance spectra at different concentrations (A) C_{Pd} from 0 M to 1.08×10^{-4} M with relevant absorbance versus concentration plot (B) and absorbance ratio plot (C), 25.0 C; (D) absorbance spectra in the 25 °C (—) – 90 °C (.....) temperature range, $C_{Pd} = 2.01\times10^{-5}$ M. NaCl 0.1 M, NaCac 2.5 mM, pH = 7.0.

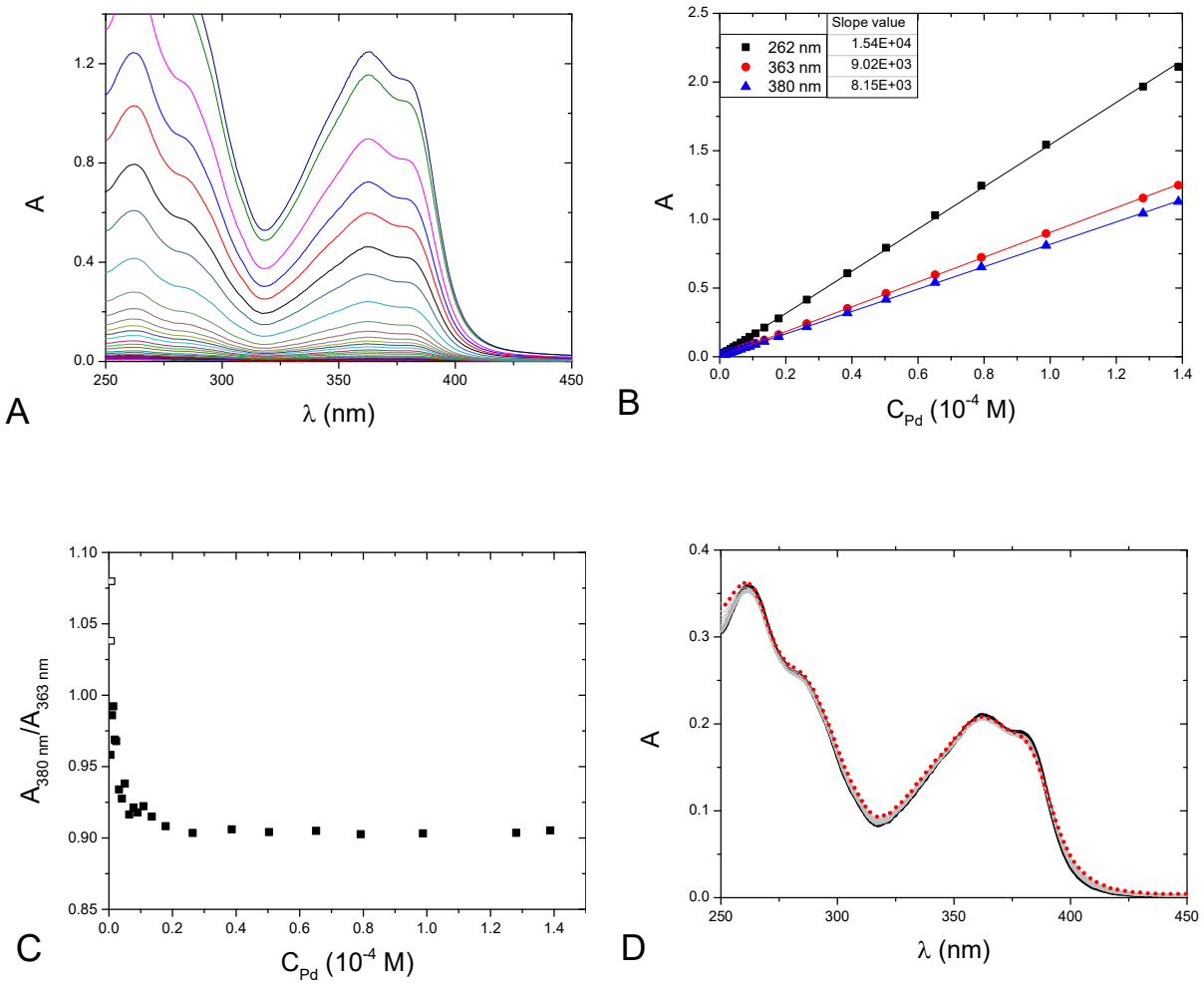

Figure S4. $[Pd(L3)](OAc)_2$: absorbance spectra at different concentrations (A) C_{Pd} from 0 M to 1.39×10^{-4} M with relevant absorbance versus concentration plot (B) and absorbance ratio plot (C), 25.0 °C; (D) absorbance spectra in the 25 °C (—) – 90 °C (.....) temperature range, $C_{Pd} = 2.64\times10^{-5}$ M. NaCl 0.1 M, NaCac 2.5 mM, pH = 7.0.

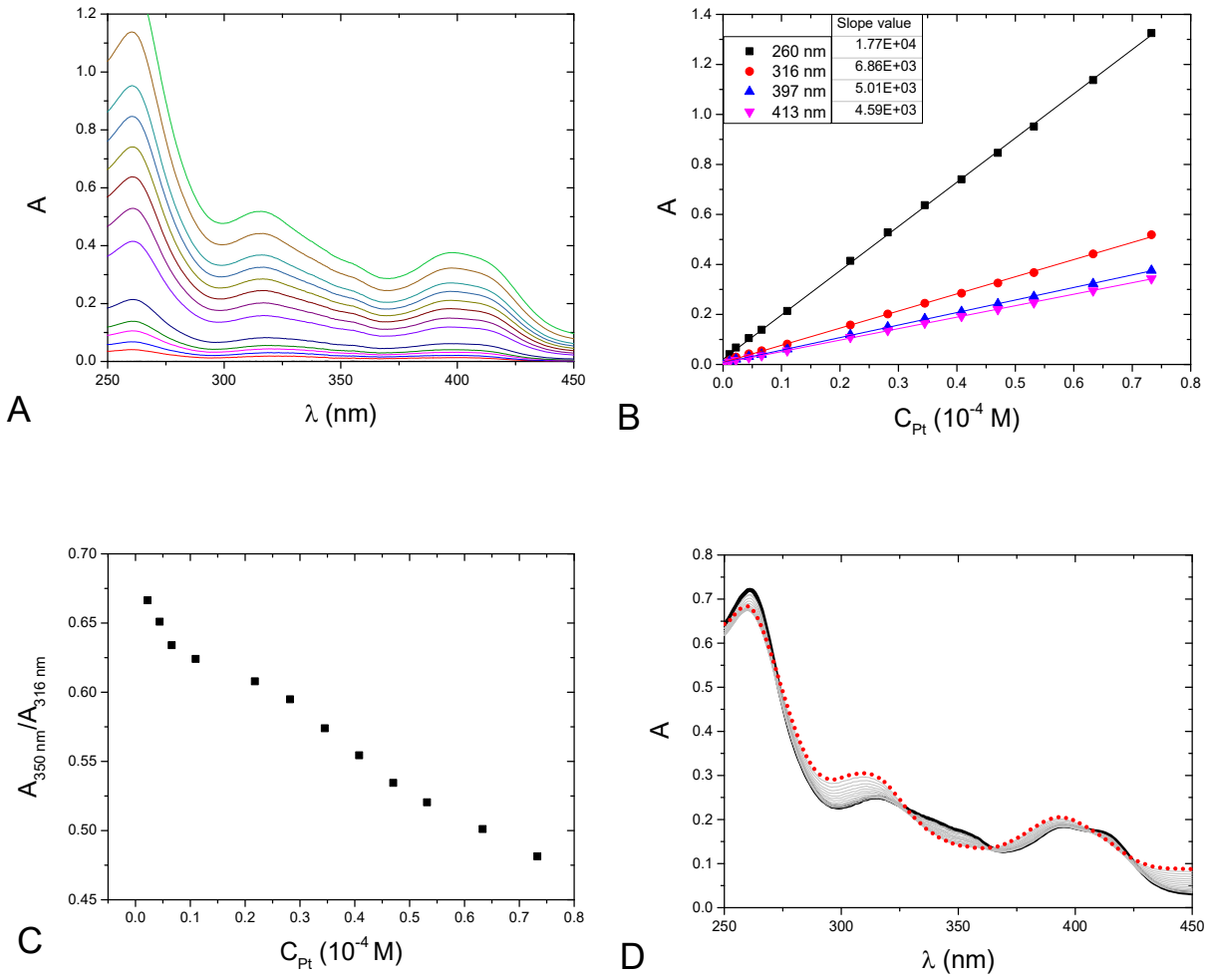

Figure S5. Complex $[Pt(H_2L1)]Cl_2$: absorbance spectra at different concentrations (A) C_{Pt} from 0 M to 7.33×10^{-5} M with relevant absorbance versus concentration plot (B) and absorbance ratio plot (C), 25.0 °C; (D) absorbance spectra in the 25 °C (—) – 90 °C (.....) temperature range, $C_{Pt} = 3.10\times10^{-5}$ M. NaCl 0.1 M, NaCac 2.5 mM, pH = 7.0.

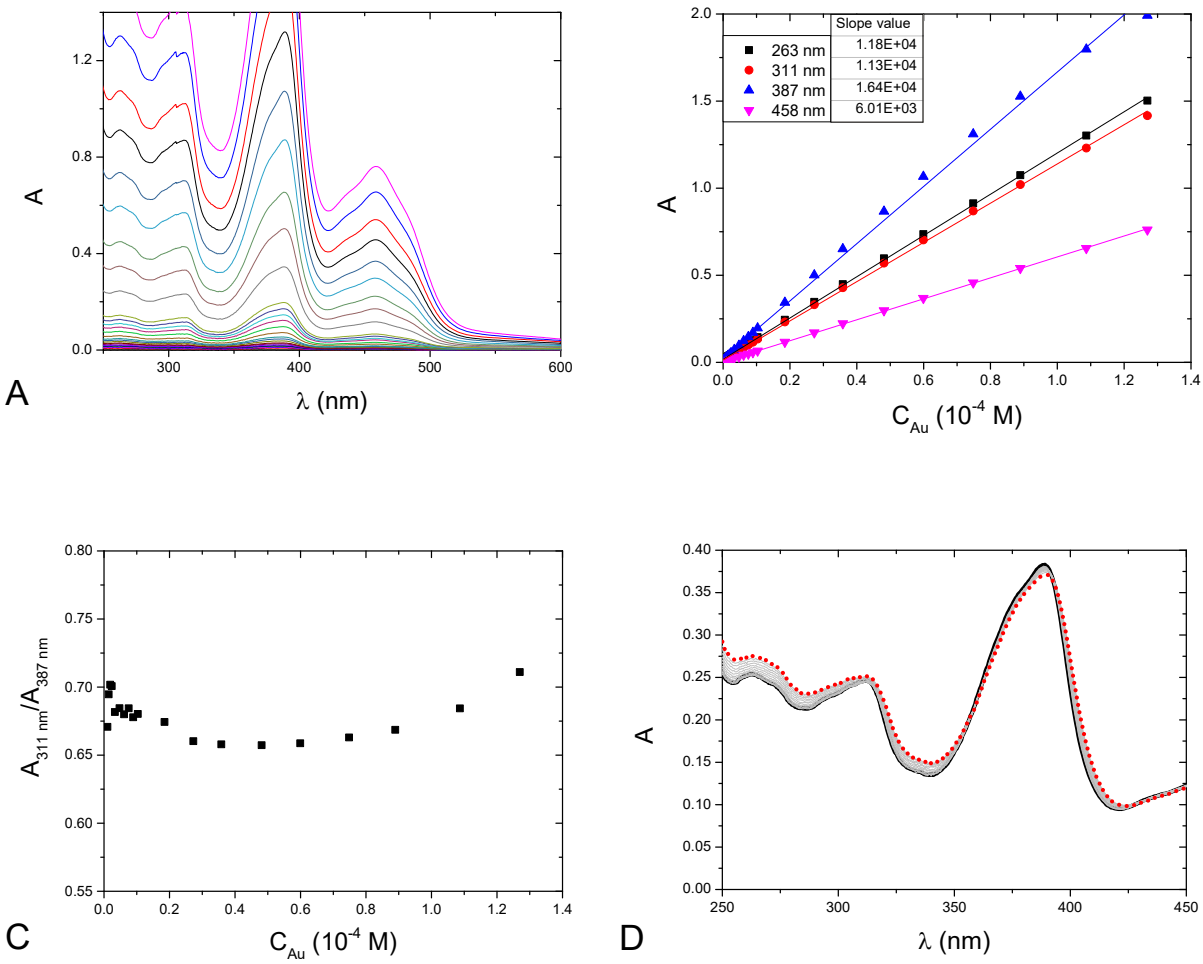

Figure S6. Complex [Au(L1)]Cl: A) Absorbance spectrum C_{Au} = 2.73×10^{-5} M, T = 25 °C; B) Absorbance versus temperature plot at different wavelengths, C_{Au} = 2.73×10^{-5} M; C) Absorbance versus concentration plot, T = 25 °C; (D) Absorbance ratio plot, T = 25 °C. Buffer: NaCl 0.1 M, NaCac 2.5 mM, pH = 7.0.

Poly(rA)2poly(rU) absorbance titrations

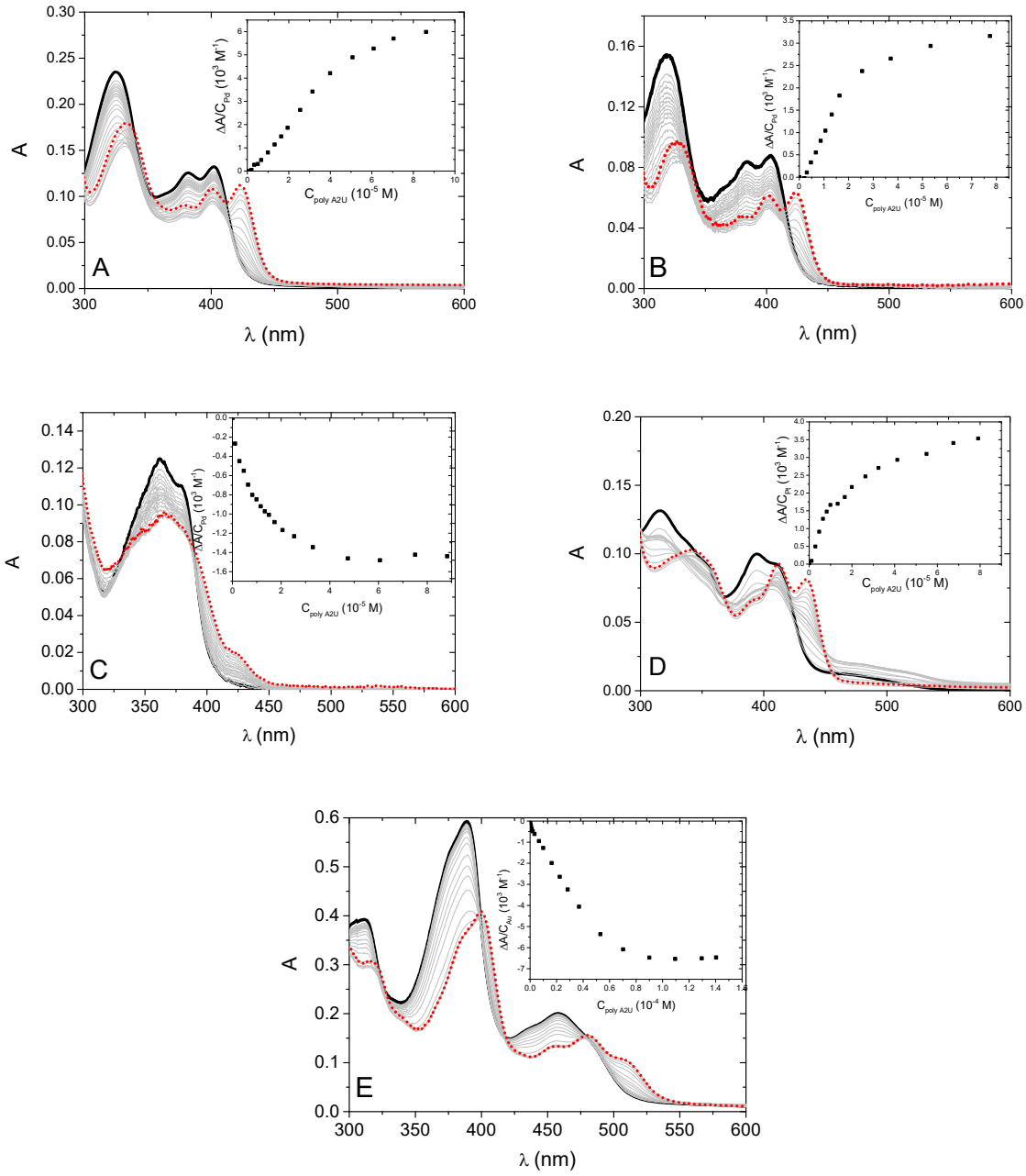

Figure S7. UV-vis titrations with poly(rA)·2poly(rU), NaCl 0.1 M, NaCac 2.5 mM, pH 7.0, 25.0 °C. (A) $[Pd(H_2L1)]Cl_2$/polyA2U system, $C_{Pd} = 1.44\times10^{-5}$ M, $C_{polyA2U}$ from 0 M (—) to 8.61×10^{-5} M (.....), the inset is the binding isotherm at λ = 425 nm; (B) $[Pd(H_2L2)]Cl_2$/polyA2U system, $C_{Pd} = 1.37\times10^{-5}$ M, $C_{polyA2U}$ from 0 M (—) to 7.74×10^{-5} M (.....), the inset is the binding isotherm at λ = 425 nm; (C) $[Pd(L3)](OAc)_2$/polyA2U system, $C_{Pd} = 1.68\times10^{-5}$ M, $C_{polyA2U}$ from 0 M (—) to 8.81×10^{-5} M (.....), the inset is the binding isotherm at λ = 369 nm; (D) $[Pt(H_2L1)]Cl_2$/polyA2U system, $C_{Pt} = 1.56\times10^{-5}$ M, $C_{polyA2U}$ from 0 M (—) to 7.91×10^{-5} M (.....), the inset is the binding isotherm at λ = 434 nm; (E) [Au(L1)]Cl/polyA2U system, $C_{Au} = 3.46\times10^{-5}$ M, $C_{polyA2U}$ from 0 M (—) to 1.4×10^{-4} M (.....), the inset is the binding isotherm at λ = 389 nm.

Melting Tests

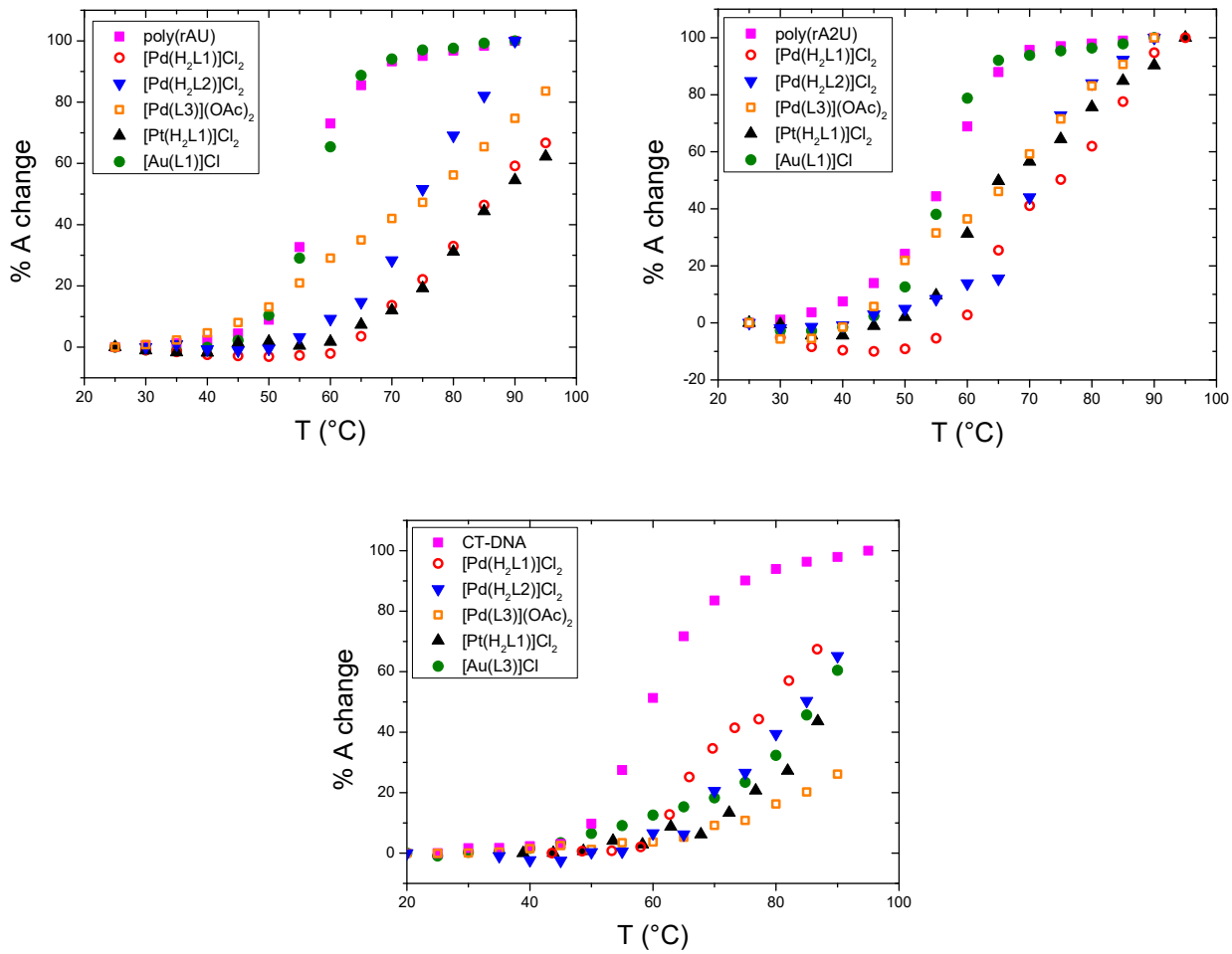

Figure S8. Melting tests for the poly(rA)poly(rU), poly(rA)2poly(rU) or CT-DNA polynucleotide alone (full squares) and for its mixtures with $[Pd(H_2L1)]^{2+}$ (open circles), $[Pd(H_2L2)]^{2+}$ (down triangles), $[Pd(L3)]^{2+}$ (open squares), $[Pt(H_2L1)]^{2+}$ (up triangles), $[Au(L1)]^{+}$ (full circles); $C_{polyrAU} = C_P$ (in base pairs) = 2.45×10^{-5} M, $C_{polyrA2U} = C_P$ (in base triplets) = 1.92×10^{-5} M, $C_{DNA} = C_P$ (in base pairs) = 2.45×10^{-5} M, r_b = complex/DNA = C_D/C_P = 1.0, buffer for RNAs NaCl 0.1 M, NaCac 2.5 mM, pH 7.0, λ = 260 nm, for CT-DNA NaCac 2.5 mM, pH 7.0, λ = 260 nm; % A change = 100*(A – A°)/(A$^{\infty}$ – A°) where A$^{\infty}$ and A° are the two absorbance values limiting the fitting sigmoid.

Table S1. Melting temperature of the polynucleotide alone (Ref) and for its mixtures with $[Pd(H_2L1)]^{2+}$, $[Pd(H_2L2)]^{2+}$, $[Pd(L3)]^{2+}$, $[Pt(H_2L1)]^{2+}$, $[Au(L1)]^{+}$. Buffer for RNAs NaCl 0.1 M, NaCac 2.5 mM, pH 7.0, for CT-DNA NaCac 2.5 mM, pH 7.0, for G-quad KCl 0.1M, LiCac 2.5 mM, pH 7.0.

	poly(rAU)	poly(rA2U)	CT-DNA	G4
Ref	57.0 ± 0.3	56.0 ± 0.3	59.8 ± 0.3	62.6 ± 0.2
$[Pd(H_2L1)]Cl_2$	> 90	74 ± 2	> 90	68.7 ± 0.5
$[Pd(H_2L2)]Cl_2$	76.7 ± 0.9	71.3 ± 0.7	82 ± 3	65.1 ± 0.2
$[Pd(L3)](OAc)_2$	83 ± 6	67 ± 3	> 90	67.9 ± 0.2
$[Pt(H_2L1)]Cl_2$	> 90	67 ± 1	> 90	65.0 ± 0.4
[Au(L1)]Cl	57.7 ± 0.2	55.9 ± 0.2	> 90	64.8 ± 0.3

Poly(rA)poly(rU) Ethidium displacement

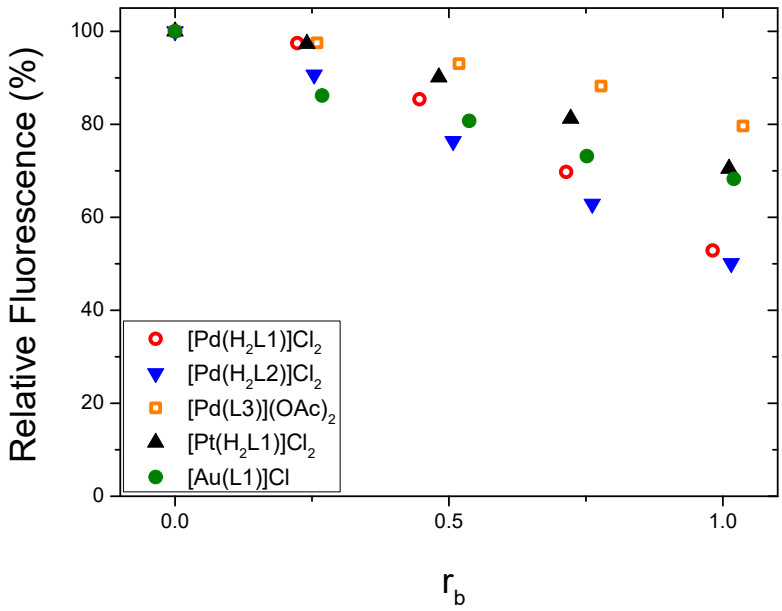

Figure S9. Ethidium bromide (EtBr) exchange tests where the metal complexes are added to EtBr-saturated poly(rA)poly(rU) where the latter adduct is strongly fluorescent only as the EtBr probe is intercalated between polynucleotide base pairs; C_{polyAU} = 1.25×10^{-4} M, C_{EtBr} = 5.84×10^{-5} M, r_b = complex/DNA = C_D/C_{polyAU}, relative fluorescence = 100*F/F° where F° is the fluorescence of the system at $r_b = 0$, λ_{ex} = 520 nm, λ_{em} = 595 nm.

DNA Absorbance titrations

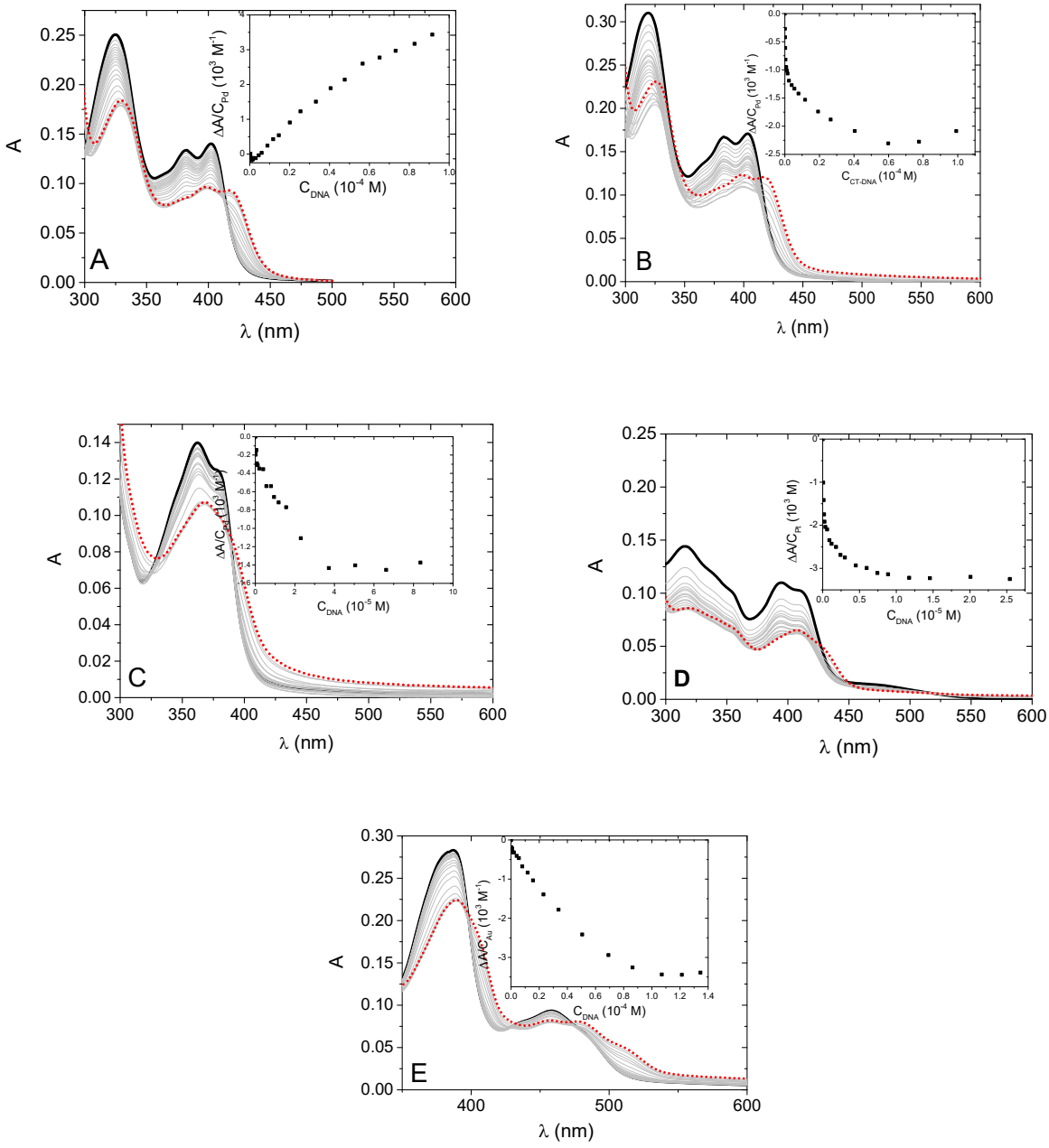

Figure S10. UV-vis titrations where increasing amounts of DNA are added to the complexes (NaCl 0.1 M, NaCac 2.5 mM, pH 7.0, 25.0 °C); (A) $[Pd(H_2L1)]Cl_2$/DNA system, C_{Pd} = 1.44×10^{-5} M, C_{DNA} from 0 M (—) to 9.15×10^{-5} M (.....), the inset is the binding isotherm at λ = 418 nm; (B) $[Pd(H_2L2)]Cl_2$/DNA system, C_{Pd} = 2.72×10^{-5} M, C_{DNA} from 0 M (—) to 1.23×10^{-4} M (.....), the inset is the binding isotherm at λ = 418 nm; (C) $[Pd(L3)](OAc)_2$/DNA system, C_{Pd} = 1.68×10^{-5} M, C_{DNA} from 0 M (—) to 8.35×10^{-5} M (.....), the inset is the binding isotherm at λ = 418 nm; (D) $[Pt(H_2L1)]Cl_2$/DNA system, C_{Pt} = 1.87×10^{-5} M, C_{DNA} from 0 M (—) to 2.54×10^{-5} M (.....), the inset is the binding isotherm at λ = 396 nm. (E) [Au(L1)]Cl/DNA system, C_{Au} = 1.74×10^{-5} M, C_{DNA} from 0 M (—) to 1.35×10^{-4} M (.....), the inset is the binding isotherm at λ = 388 nm.

DNA Ethidium displacement and viscometric tests

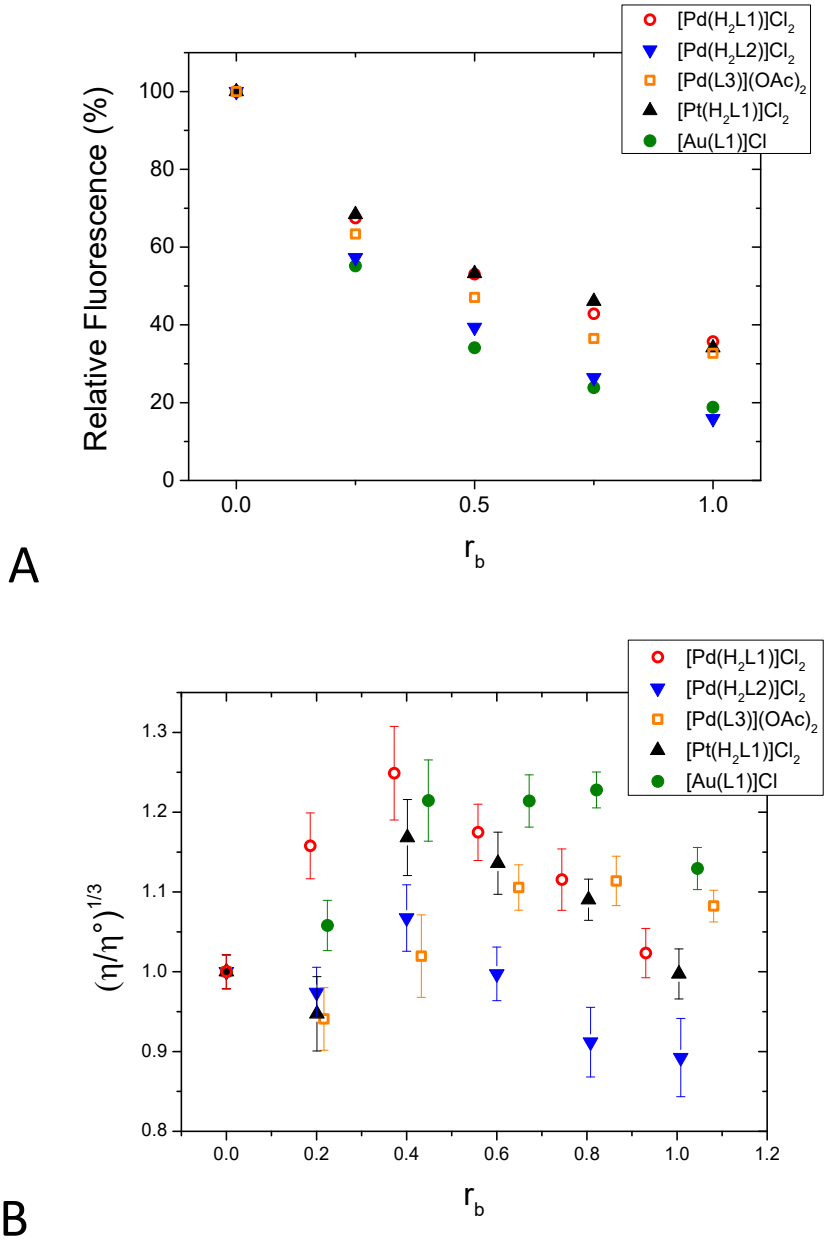

Figure S11. (A) Ethidium bromide (EtBr) exchange tests where the metal complexes are added to EtBr-saturated DNA where the latter adduct is strongly fluorescent only as the EtBr probe is intercalated between polynucleotide base pairs; C_{DNA} = 1.49×10^{-4} M, C_{EtBr} = 6.11×10^{-5} M, r_b = complex/DNA = C_D/C_{DNA}, relative fluorescence = 100*F/F° where F° is the fluorescence of the system at r_b = 0, λ_{ex} = 520 nm, λ_{em} = 595 nm. (B) Viscosity of DNA with increasing amount of metal complexes; C_{DNA} = 1.2×10^{-4} M, r_b = complex/DNA, $(\eta/\eta°)^{1/3}$ = $(t_{complex} - t_{DNA})/(t_{DNA} - t_{solvent})$. For both panels NaCl 0.1 M, NaCac 2.5 mM, 25.0°C, pH 7.0.

Circular Dichroism spectra of $[Pd(H_2L1)]Cl_2$/DNA and $[Pt(H_2L1)]Cl_2$/DNA

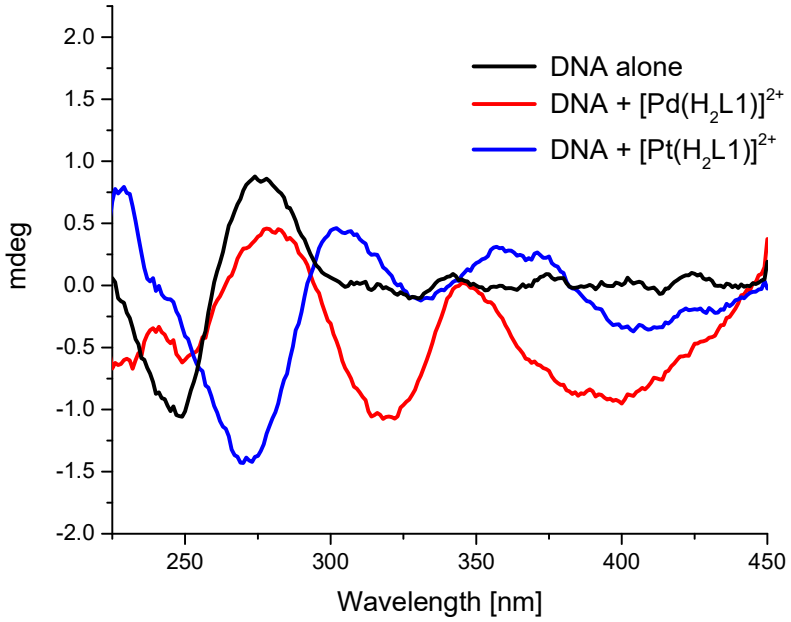

Figure S12. Circular dichroism spectra of DNA alone and in mixture with wither $[Pd(H_2L1)]^{2+}$ or $[Pt(H_2L1)]^{2+}$ metal complexes. C_{DNA} = 1.0×10^{-5} M; C_{Pd} = C_{Pt} = 2.2×10^{-5} M; NaCl 0.1 M, NaCac 2.5 mM, T = 25.0 °C, pH 7.0.

G-quadruplex absorbance titrations

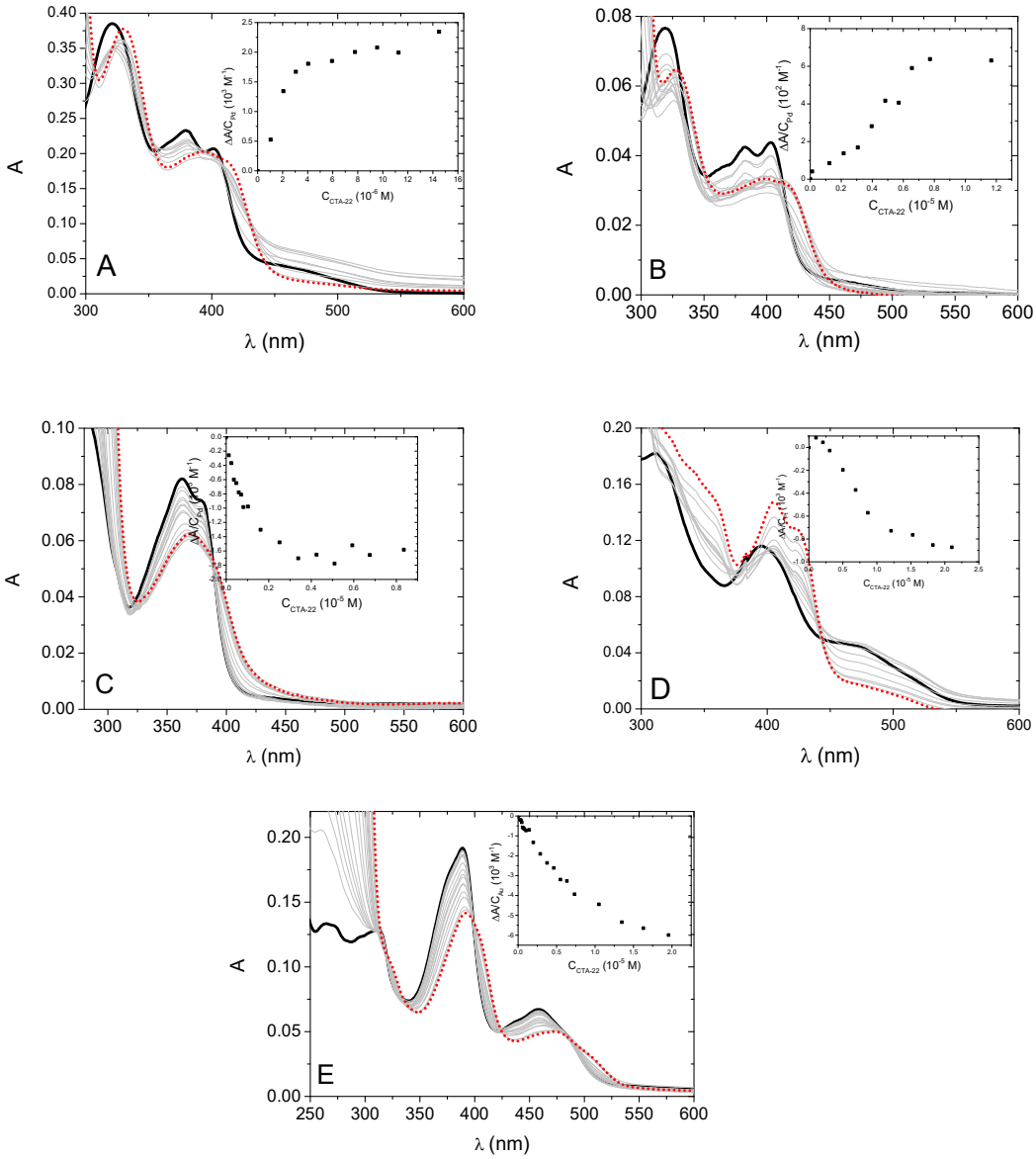

Figure S13. UV-vis titrations with G-quadruplex (CTA-22), KCl 0.1 M, LiCac 2.5 mM, pH 7.0, T = 25.0 °C. (A) $[Pd(H_2L1)]Cl_2$/CTA-22 system, C_{Pd} = 2.87×10^{-5} M, C_{CTA-22} from 0 M (—) to 1.45×10^{-5} M (.....), the inset is the binding isotherm at λ = 425 nm; (B) $[Pd(H_2L2)]Cl_2$/polyA2U system, C_{Pd} = 9.08×10^{-6} M, C_{CTA-22} from 0 M (—) to 1.17×10^{-5} M (.....), the inset is the binding isotherm at λ = 422 nm; (C) $[Pd(L3)](OAc)_2$/polyA2U system, C_{Pd} = 9.53×10^{-6} M, C_{CTA-22} from 0 M (—) to 8.35×10^{-6} M (.....), the inset is the binding isotherm at λ = 369 nm; (D) $[Pt(H_2L1)]Cl_2$/polyA2U system, C_{Pt} = 3.10×10^{-5} M, C_{CTA-22} from 0 M (—) to 2.10×10^{-5} M (.....), the inset is the binding isotherm at λ = 434 nm; (E) [Au(L1)]Cl/polyA2U system, C_{Au} = 8.68×10^{-6}, CTA22 from 0 M (—) to 1.96×10^{-5} M (...), the inset is the binding isotherm at λ = 389 nm.

G-quadruplex ESI mass spectra

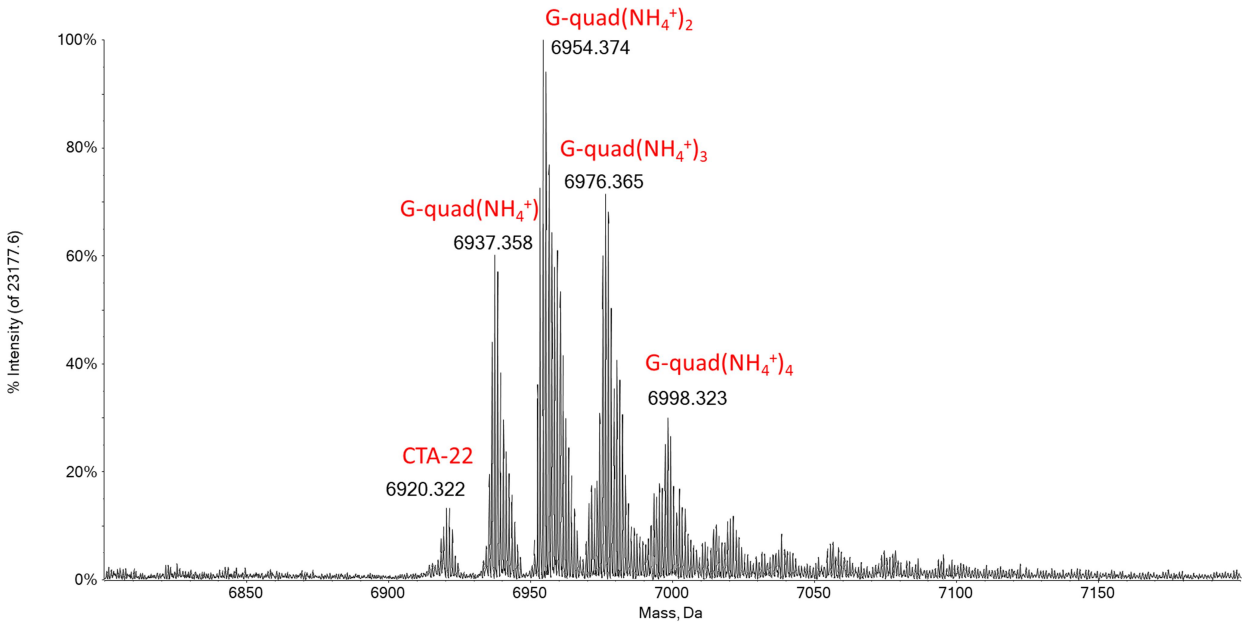

Figure S14. Deconvoluted ESI mass spectra of 10^{-6} M CTA-22 annealed in 100 mM ammonium acetate solution (pH 7.0) and recorded in the presence of 60% EtOH.

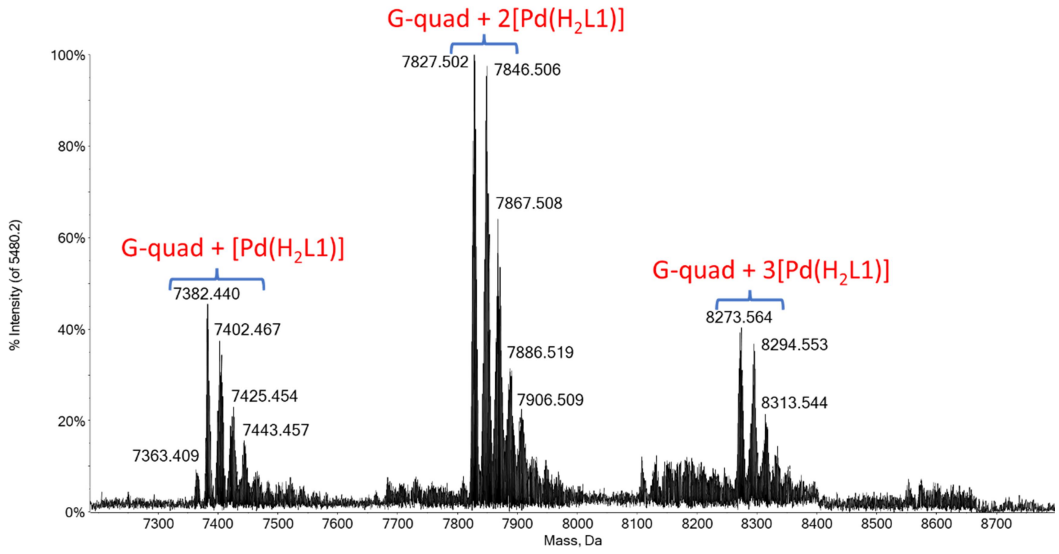

Figure S15. Deconvoluted ESI mass spectrum of 10^{-6} M G-quadruplex incubated for 24 h with $[Pd(H_2L1)]Cl_2$ in 100 mM ammonium acetate solution (pH 7.0) and in the presence of 60% EtOH. 3:1 metal complex/G-quad molar ratio.

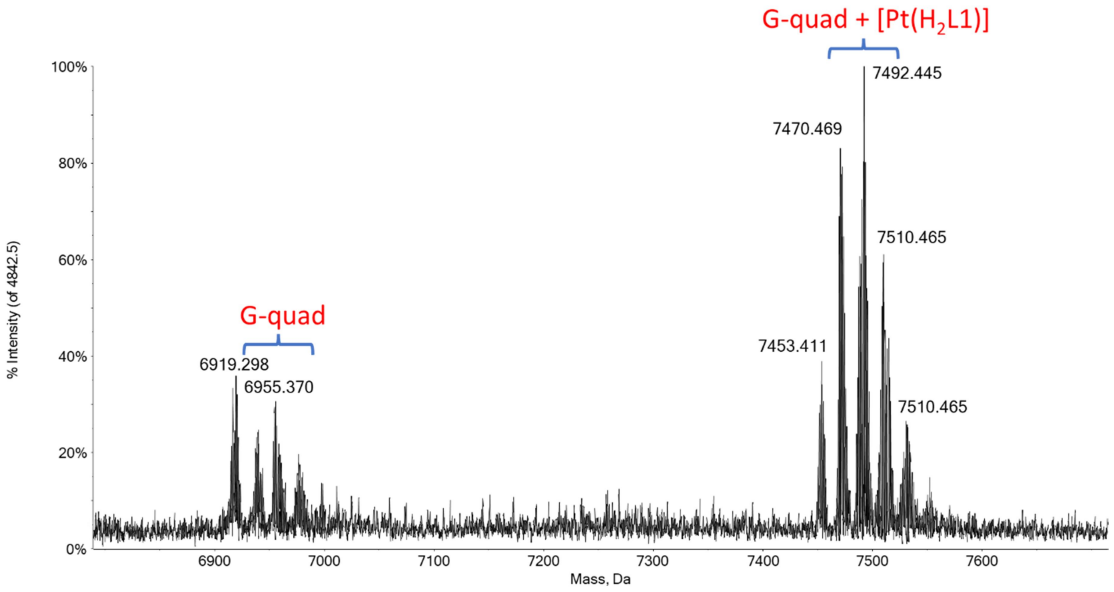

Figure S16. Deconvoluted ESI mass spectrum of 10^{-6} M G-quadruplex incubated for 24 h with $[Pt(H_2L1)]Cl_2$ in 100 mM ammonium acetate solution (pH 7.0) and in the presence of 60% EtOH. 3:1 metal complex/G-quad molar ratio.

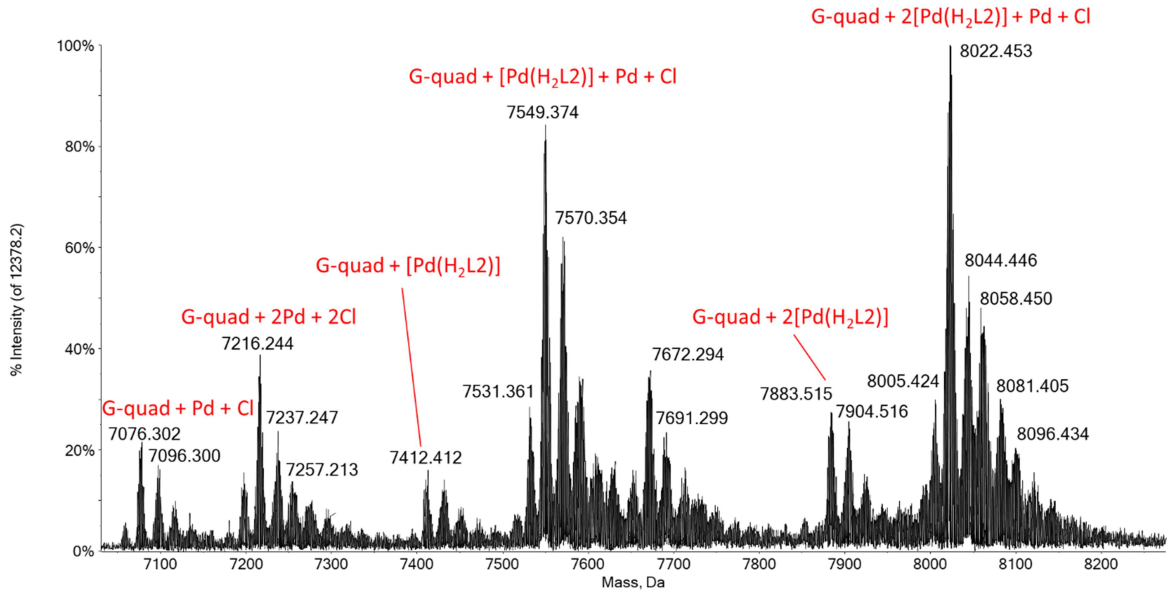

Figure S17. Deconvoluted ESI mass spectrum of 10^{-6} M G-quadruplex incubated for 24 h with $[Pd(H_2L2)]Cl_2$ in 100 mM ammonium acetate solution (pH 7.0) and in the presence of 60% EtOH. 3:1 metal complex/G-quad molar ratio.

RNA-4WJ absorbance titrations

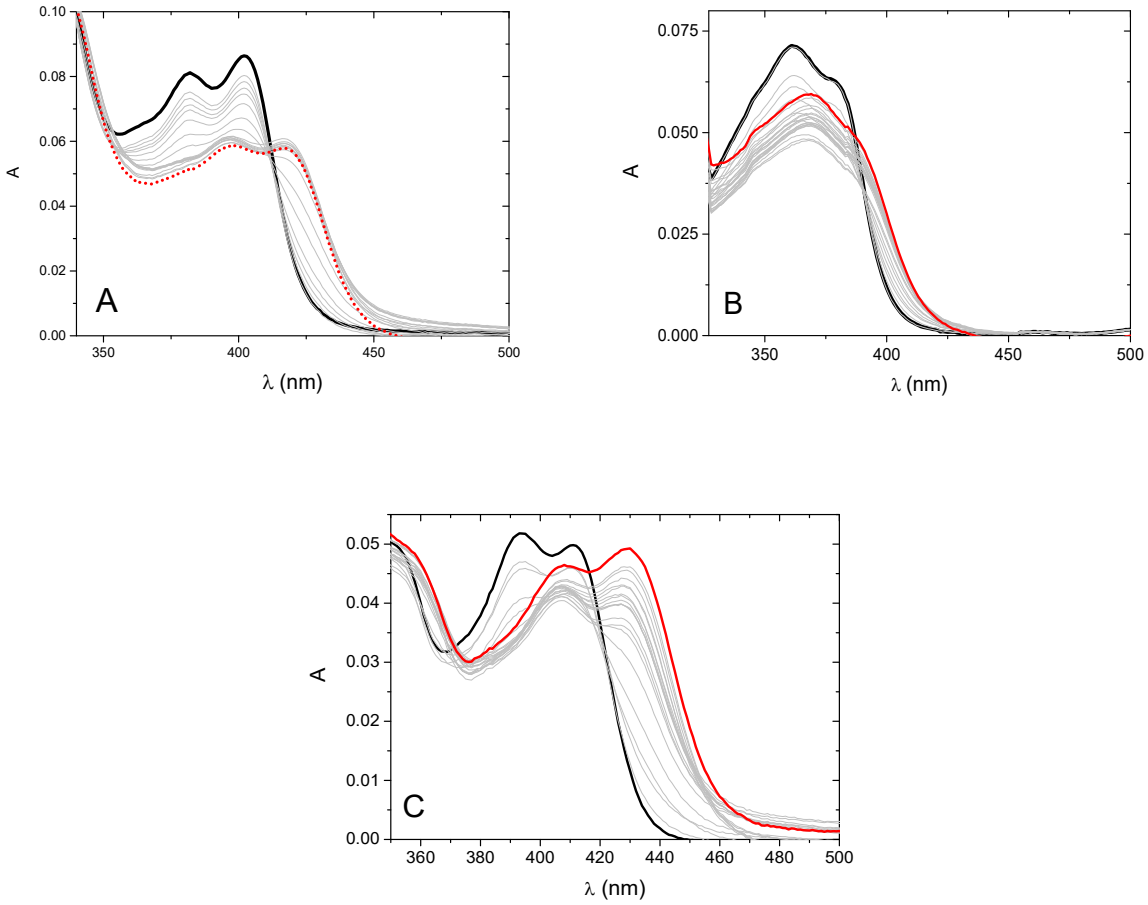

Figure S18. UV-vis titrations with RNA-4WJ, $CaCl_2$ 182 µM, pH 7.0, T = 25.0 °C. (A) $[Pd(H_2L1)]Cl_2$/RNA-4WJ system, $C_{Pd} = 8.76\times10^{-6}$ M, C_{RNA4WJ} from 0 M (—) to 6.20×10^{-6} M (.....); (B) $[Pd(L3)](OAc)_2$/RNA-4WJ system, $C_{Pd} = 9.06\times10^{-6}$ M, C_{RNA4WJ} from 0 M (—) to 7.58×10^{-6} M (.....); (C) $[Pt(H_2L1)]Cl_2$/RNA-4WJ system, $C_{Pt} = 8.75\times10^{-6}$ M, C_{RNA4WJ} from 0 M (—) to 6.16×10^{-6} M (.....).

RNA-4WJ melting tests

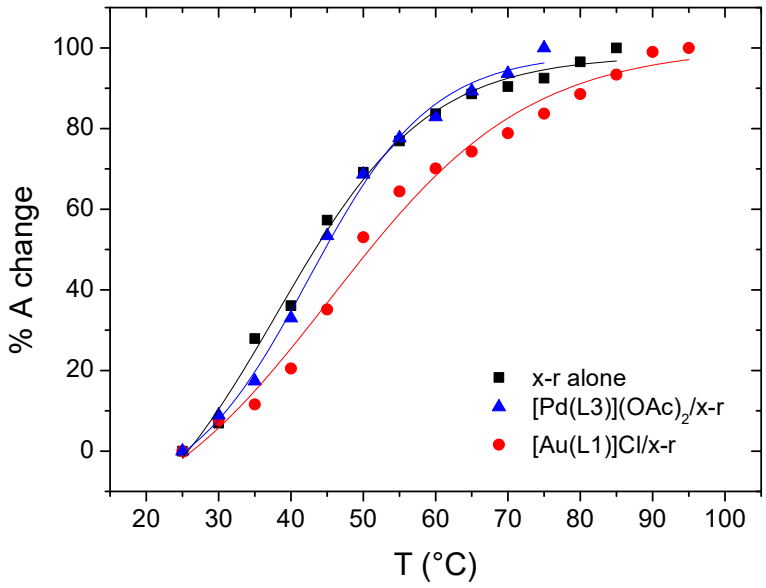

Figure S19. Melting profiles for the coupled x-r strands alone, for the $[Pd(L3)](OAc)_2$/x-r strands system and for the [Au(L1)]Cl/x-r strands system; $C_{x\text{-}r}$ = 1.03x10^{-5} M, C_{Pd} = 1.86×10^{-5} M, C_{Au} = 1.83×10^{-5} M; C_{CaCl2} = 182 µM, pH 7.0, λ = 260 nm; % A change = 100*(A – A°)/(A$^{\infty}$ – A°) where A$^{\infty}$ and A° are the two absorbance values limiting the fitting sigmoid.